Molecular Neurobiology (2019) 56:6168–6183
https://doi.org/10.1007/s12035-019-1507-4

Pathological Alterations of Tau in Alzheimer's Disease and 3xTg-AD Mouse Brains

Longfei Li[1,2] · Yanli Jiang[1,2] · Wen Hu[2] · Yunn Chyn Tung[2] · Chunling Dai[2] · Dandan Chu[1] · Cheng-Xin Gong[2] · Khalid Iqbal[2] · Fei Liu[2]

Received: 12 November 2018 / Accepted: 23 January 2019 / Published online: 8 February 2019

Abstract

Microtubule-associated protein tau in Alzheimer's disease (AD) brain is hyperphosphorylated, truncated, and aggregated into neurofibrillary tangles. Oligomeric and hyperphosphorylated tau (Oligo-tau) isolated from AD brain captures and templates normal tau into filaments both in vitro and in vivo; this prion-like activity is believed to be responsible for the progression of neurofibrillary pathology in AD. The 3xTg-AD mouse model develops both Aβ and tau pathologies and thus gains popularity in preclinical studies of AD. Despite the histopathological similarity of the 3xTg-AD model to AD, biochemical authenticity of tau alterations in this model remains elusive. To investigate the biochemical basis of tau pathology in 3xTg-AD brain, we here compared pathological alterations of tau in the aged 3xTg-AD brain to those in AD brain. We found that in contrast to substantial high molecular weight smear tau (HMW-tau) lacking the N-terminal portion and hyperphosphorylated at multiple sites in AD brain, tau in 3xTg-AD mouse brain showed no detectable HMW-tau or truncation but slightly increased phosphorylation when normalized with total tau. In addition, AT8 immunostaining exhibited filamentous tau inclusions in AD brain, but predominantly truffle-like morphology in aged 3xTg-AD mouse brain. Further, Oligo-tau isolated from 3xTg-AD mice showed minimal potency in capturing tau in vitro and seeding tau aggregation in cultured cells when compared to AD Oligo-tau. These findings suggest that the alterations of tau in 3xTg-AD mouse brain differ from those in AD brain. In 3xTg-AD mice, the lack of N-terminal truncation, scarce SDS/reducing reagent-resistant HMW-tau, and minimal hyperphosphorylation may collectively result in low potency in prion-like activity of the Oligo-tau.

Keywords Alzheimer's disease · 3xTg-AD mice · Tau · Phosphorylation · Truncation · Prion-like properties

Introduction

Alzheimer's disease (AD) is multifactorial and involves different etiopathogenic mechanisms [1, 2]. Histopathologically, AD is characterized by numerous intraneuronal neurofibrillary tangles (NFTs), extracellular deposits of β-amyloid as cores of neuritic (senile) plaques, and neurodegeneration of the brain, especially the hippocampus and the neocortex. Clinico-pathological correlation studies have shown that the number of NFTs, but not of amyloid plaques, correlates with the degree of dementia in AD patients [3–6] .

NFTs are composed of hyperphosphorylated and aggregated microtubule-associated protein tau (MAPT) [7, 8]. The biological activity of tau is regulated by its degree of phosphorylation. In AD brain, tau is abnormally hyperphosphorylated, truncated, and aggregated to form paired helical filaments (PHFs)/NFTs [9–11]. Hyperphosphorylation of tau inhibits its activity in promoting microtubule assembly [10, 12]. Furthermore, phosphorylation and truncation of tau promote its aggregation [13, 14]. Unlike normal tau, the hyperphosphorylated and oligomeric tau from AD brain (AD p-tau) captures normal tau and templates it into filaments [10]; this phenomenon was recently called a prion-like property, which might be the molecular basis of the

Longfei Li and Yanli Jiang contributed equally to this work.

✉ Fei Liu
feiliu63@hotmail.com

[1] Key Laboratory of Neuroregeneration of Jiangsu and Ministry of Education of China, Co-innovation Center of Neuroregeneration, Nantong University, 19 Qixiu Road, Nantong 226001, Jiangsu, China

[2] Department of Neurochemistry, Inge Grundke-Iqbal Research Floor, New York State Institute for Basic Research in Developmental Disabilities, 1050 Forest Hill Road, Staten Island, NY 10314, USA

propagation of tau pathology [15–17]. The prion-like seeding and templating of normal tau by AD p-tau in vitro are inhibited by its prior dephosphorylation [10, 11].

NFTs are initially seen in the entorhinal cortex, then appear in the hippocampal formation and some parts of the neocortex, followed by most of the neocortex. This process was identified by Braak and Braak and named the Braak Stages [18, 19]. Thus, tau pathology in AD develops progressively in anatomically connected regions of the brain. Similar to steps in propagation of tau pathology seen in AD, the propagation of tau pathology was induced experimentally by injection of tau aggregates isolated from AD brains or produced in vitro into mouse brain [20–26]. In addition, tau aggregation is induced in cultured cells by adding tau aggregates into the culture medium [27, 28]. Thus, aggregated tau seeds template tau aggregation in vitro and in vivo in a prion-like fashion [15, 29], the basis of the spreading of tau pathology in vivo.

The 3xTg-AD mouse is a widely used AD mouse model; it contains three mutations (APP Swedish, MAPT P301L, and PSEN1 M146V) in the brain [30] and develops Aβ plaques and tau pathology in the hippocampus from 6 months of age [31]. However, a comprehensive comparison of the pathological alterations of tau in AD and 3xTg-AD mouse brains is not available. Here, we analyzed the pathological changes of tau in AD brain and 3xTg-AD mouse brain by using Western blots and by determining the prion-like activity of their cytosolic/oligomeric tau (Oligo-tau). We found that tau in AD brain was abnormally hyperphosphorylated, truncated at the N-terminus, and exhibited high molecular tau (HMW-tau) smear in Western blots, whereas these alterations were not seen in the aged 3xTg-AD mouse brains. Oligo-tau from AD brains, but not from aged 3xTg-AD mouse brains, was abnormally hyperphosphorylated, truncated, and presented as HMW-tau smear. Oligo-tau from AD brain was much more potent in capturing tau in vitro and in seeding tau aggregation in cultured cells than that from 3xTg-AD mouse brain.

Materials and Methods

Human Brain Tissue

Frozen frontal cortices from autopsied and histopathologically confirmed AD and age-matched normal human brains (Table 1) were obtained without identification of donors from the Sun Health Research Institute Donation Program (Sun City, AZ, USA). Brain samples were stored at − 80 °C until used. The use of autopsied frozen human brain tissue was in accordance with the National Institutes of Health guidelines and was exempted by the Institutional Review Board (IRB) of New York State Institute for Basic Research in Developmental Disabilities because "the research does not involve intervention or interaction with the individuals" nor "is the information individually identifiable."

Animals

The homozygous 3xTg-AD mouse harboring $PS1_{M146V}$, APP_{Swe}, and tau_{P301L} transgenes and the wild type (WT) control mouse (a hybrid of 129/Sv and C57BL/6 mice) were initially obtained from Dr. F.M. LaFerla [30] through the Jackson Laboratory (New Harbor, ME, USA; https://www.jax.org/strain/004807). Tau knockout mice (Tau_{KO}) were purchased from the Jackson Laboratory [34]. Mice were housed (four to five animals per cage) with a 12/12 h light/dark cycle and with ad libitum access to food and water. The housing, breeding, and animal experiments were in accordance with the approved protocol according to the PHS Policy on Human Care and Use of Laboratory animals. The female 3xTg-AD mice were reported to develop amyloid plaques and tau pathology in the hippocampus from 6 months of age [31], and the pathologies are predominantly restricted to the hippocampus, amygdala, and cerebral cortex [30, 35]. Unlike females, 3xTg-AD males show inconsistent and weak pathology [36–38], and hence only 18–22 months old female 3xTg-AD (~ 31 g body weight), WT (~ 36 g body weight), and Tau_{KO} animals were used in the present study.

Cell Culture

HEK-293FT cells and HeLa cells were maintained in Dulbecco's modified Eagle's medium (DMEM) supplemented with 10% fetal bovine serum (FBS) (ThermoFisher Scientific, Waltham, MA) at 37 °C (5% CO_2). Transfections were performed with Fugene HD (Promega, Madison, WI, USA) according to the manufacturer's instructions.

Western Blots and Immuno-dot Blots

The brain tissue was homogenized in cold buffer consisting of 50 mM Tris-HCl, pH 7.4, 8.5% sucrose, 2.0 mM EDTA, 10 mM β-mercaptoethanol, 1.0 mM orthovanadate, 50 mM NaF, 1.0 mM 4-(2-aminoethyl) benzenesulfonyl fluoride hydrochloride (AEBSF), and 10 μg/ml each of aprotinin, leupeptin, and pepstatin. Brain homogenates were diluted in 2× Laemmli SDS sample buffer at 1:1 ratio, followed by boiling for 5 min. Protein concentration was measured using the Pierce™ 660nm Protein Assay kit (ThermoFisher Scientific). Samples were subjected to 7.5% SDS-PAGE and transferred onto polyvinylidene fluoride membrane (MilliporeSigma, Burlington, MA).

For immune-dot-blot, different amounts of Oligo-tau samples were applied onto nitrocellulose membrane (Schleicher and Schuell, Keene, NH, USA) at 5 μl per grid of 7 × 7 mm in

Table 1 Human brain tissue of Alzheimer's disease (AD) and control (Con) cases used in this study

Case	Age at death (year)	Gender	PMI[a](h)	Braakstage[b]	Tangle scores[c]
AD 1	83	F	3.0	VI	12.4
AD 2	74	M	2.75	VI	14.66
AD 3	79	F	1.5	VI	14.66
AD 4	73	F	2.0	V	15.00
AD 5	81	M	3.0	V	11.00
AD 6	76	M	2.33	VI	15.00
AD 7	72	M	2.5	VI	15.00
AD 8	74	F	2.83	VI	15.00
AD 9	76	M	4.0	V	15.00
AD 10	78	M	1.83	VI	15.00
Mean ± SD	76.60 ± 3.60		2.57 ± 0.71		14.27 ± 1.40
Con 1	85	M	2.5	II	4.25
Con 2	85	F	2.75	II	5.0
Con 3	82	F	2.0	II	4.25
Con 4	70	F	2.0	I	0.00
Con 5	73	M	2.0	III	2.75
Con 6	78	M	1.66	I	0.00
Con 7	80	M	2.16	II	1.00
Con 8	83	F	3.25	I	0.75
Con 9	82	F	2.25	II	3.50
Mean ± SD	79.78 ± 5.24		2.29 ± 0.48		2.39 ± 1.97

[a] *PMI* postmortem interval; [b] Neurofibrillary pathology was staged according to Braak and Braak [32]; [c] Tangle score was a density estimate and was designated as none, sparse, moderate, or frequent (0, 1, 2, or 3 for statistics), as defined according to CERAD Alzheimer's disease criteria [33]. Five areas (frontal, temporal, parietal, hippocampal, and entorhinal) were examined, and the scores were combined for a maximum of 15

size. The blot was placed in a 37 °C oven for 1 h (hour) to allow the protein to bind to the membrane.

The membrane was subsequently blocked with 5% fat-free milk-TBS (Tris-buffered saline) for 30 min, incubated with primary antibodies (Table 2) in TBS overnight, washed with TBST (TBS with 0.05% Tween 20), incubated with HRP-conjugated secondary antibody for 2 h at RT, washed with TBST, incubated with the ECL Western Blotting Substrate (ThermoFisher Scientific) and exposed to HyBlot CL® autoradiography film (Denville Scientific Inc., Holliston, MA). Specific immunostaining was quantified by using the Multi Gauge software V3.0 from Fuji Film (Minato, Tokyo, Japan).

Preparation of Oligomeric Tau Aggregates

Oligomeric tau aggregates were isolated from the cerebral cortex of frozen autopsied AD brains or 22-month-old 3xTg-AD mouse brains as described by us previously [25]. Briefly, 10% brain homogenate prepared in buffer as above was centrifuged at 27,000×*g* for 30 min. The supernatant was further centrifuged at 235,000×*g* for 45 min and the resulting pellet, i.e., oligomeric tau aggregates (Oligo-tau), was collected and washed three times and then resuspended in normal saline. The Oligo-tau was probe-sonicated for 10 min at 20% Power.

Tau Capture Assay

$Tau_{151–391}$ tagged with HA at the N-terminus was overexpressed in HEK-293FT cells for 48 h. The cells were lysed in PBS (phosphate-buffered saline) containing 50 mM NaF, 1 mM Na_3VO_4, 1.0 mM AEBSF, and 10 μg/ml each of aprotinin, leupeptin, and pepstatin by probe sonication. The cell lysate was centrifuged for 10 min at 10,000×*g*. The supernatant containing HA-$tau_{151–391}$ was stored at − 80 °C until used.

The amount of tau isolated from AD and from 3xTg-AD mouse brains was determined by immune-dot blots as described previously [43]. Same amounts of Oligo-tau from AD brains and from 3xTg-AD mouse brains were dotted on nitrocellulose membrane after serial dilution in TBS and dried at 37 °C for 1 h. The membrane was blocked with 5% milk in TBS for 2 h and incubated with above cell extract containing HA-$tau_{151–391}$ overnight. After washing three times with TBST, the membrane was incubated with polyclonal anti-HA (1:2000) in 5% milk in TBST overnight and processed as immune-dot blot as described above.

Table 2 Antibodies used in the present study

Antibody	Type	Specificity	Species	Source/reference (catalog/lot no.)
111E	Poly-	Pan tau	R	Homemade [39]
113E	Poly-	Pan tau (a.a.19–32)	R	Homemade
R134d	Poly-	Pan tau	R	Homemade [40]
92E	Poly-	Pan tau	R	Homemade [39]
43D	Mono-	Pan tau (a.a. 6–18)	M	Homemade [41]
63B	Mono-	Pan tau (a.a. 74–103)	M	Homemade
HT7	Mono-	Pan tau (a.a.159–163)	M	ThermoFisher Scientific (MN10000/LK152163)
39E10	Mono-	Pan tau (a.a.189–195)	M	Homemade
TAU5	Mono-	Pan tau (a.a. 210–230)	M	Millipore (MAB361/1816394)
77G7	Mono-	Pan tau (a.a. 244–368)	M	Homemade
Tau46	Mono-	Pan tau (a.a. 404–421)	M	Invitrogen (13-6400/643302A)
Anti-pS199	Poly-	p-tau (S199)	R	Invitrogen (44734G/0300A)
AT8	Mono-	p-tau (S202/T205)	M	ThermoFisher Scientific (MN1020/PI205175)
Anti-pT205	Poly-	p-tau (T205)	R	Invitrogen (44738G/RD214239)
Anti-pT212	Poly-	p-tau (T212)	R	Invitrogen (44740G/1709582A)
Anti-pS214	Poly-	p-tau (S214)	R	Invitrogen (44742G/0500B)
Anti-pT217	Poly-	p-tau (T217)	R	Invitrogen (44744/785771A)
Anti-pS262	Poly-	p-tau (S262)	R	ThermoFisher Scientific (44-750G/0204)
PHF1	Mono-	p-tau (S396/S404)	M	Dr. Peter Davies
R145	Poly-	p-tau (S422)	R	Homemade [42]
Anti-HA	Poly-	HA	R	Sigma (H6908/110M4845)
GAPDH	Poly-	GAPDH	R	Sigma (G9545/015M4824V)

Abbreviations: *Mono* monoclonal, *Poly-* polyclonal, *p-* phosphorylated, *M* mouse, *R* rabbit

Immunohistochemistry

Free-floating sections, 40 μm in thickness, of frontal cortex of AD (Braak stage V) and brains of 22-month-old female 3xTg-AD mice were washed with PBS, subsequently subjected to permeabilization and removal of endogenous peroxidase activity, blocked with normal goat serum, and then incubated with mouse monoclonal anti-pS^{202}/pT^{205}-tau (AT8, 0.2 μg/ml) overnight at 4 °C. After washing in PBS, the sections were incubated with horseradish peroxidase–conjugated goat-anti-mouse IgG (1:2000, Jackson ImmunoResearch) at room temperature for 2 h, washed and developed in 0.05% diaminobenzidine plus 0.015% hydrogen peroxide. Sections were then mounted on microscopic slides, air-dried overnight, rehydrated and counterstained with Mayer's hematoxylin, dehydrated in ascending concentrations of ethanol, cleared in Histoclear, and coverslipped. Photomicrogaphs were taken on a Nikon 90i digital microscope. Non-immunized normal goat serum in replace of AT8 was used as a negative control for immunostaining.

Oligo-tau Seeded Tau Aggregation in Cultured Cells

HeLa cells were transfected with pCI/HA-$tau_{151–391}$ with FuGENE HD to express $tau_{151–391}$. Same amount of Oligo-tau from AD brains or from 3xTg-AD mouse brains was mixed with Lipofectamin 2000 (0.31% in Opti-MEM) (ThermoFisher Scientific) in 20 μl for 20 min at RT. The Oligo-tau/Lipofectamin was added into the cell cultures after 6 h transfection. The cells were fixed for 15 min with 4% PFA in phosphate buffer 42 h after Oligo-tau treatment, washed with PBS and treated with 0.3% Triton in PBS for 15 min at RT. After blocking with 5% newborn goat serum, 0.1% Triton X-100, and 0.05% Tween 20 in PBS for 30 min, the cells were incubated with polyclonal anti-HA in blocking solution overnight at 4 °C, washed with PBS, and incubated with Alexa 488-conjugated-second antibody for 2 h at RT. TO-PRO-3 iodide (5 mg/ml) was used to stain nuclei. After washing with PBS, the cells were mounted with ProLong™ Gold antifade reagent (ThermoFisher Scientific) and observed with a Nikon confocal microscope.

Statistical Analysis

Comparison between two groups was analyzed by unpaired two-tailed Student's *t* test (for data with normal distribution) or Mann-Whitney *U* test (for data with non-normal distribution). For multiple comparisons, one-way analysis of variance (one-way ANOVA) followed by Tukey's post hoc test or two-

way ANOVA followed by Sidak's multiple comparisons test was used. For analysis of the correlation, Pearson (data with normal distribution) correlation coefficient was calculated. The data are presented as the mean ± S.D. $p < 0.05$ was considered statistically significant.

Results

High Molecular Weight Tau Smear (HMW-tau) Is Seen in AD but Not in 3xTg-AD Mouse Brains in Western Blots

To compare the pathological alterations of tau in AD and 3xTg-AD mice, brain homogenates from the frontal cortices of AD and control human cases and from the fore brain of 18-month-old 3xTg-AD and wild type (WT) female mice were analyzed by Western blots developed with polyclonal pan-tau antibodies, 113e, R134d, 92e, and 111e, raised in our laboratory since tau pathology became significantly worse as the mice aged [31]. We found that brain homogenates from control, AD, WT mice, and 3xTg-AD mice were immunoreactive to 111e, R134d, and 92e. As a negative control, we included brain homogenates from two tau knockout (tau_{KO}) female mice, which showed no immunoreaction and thus confirmed the specificity of these pan-tau antibodies. In the blot developed with 113e, which was raised with 19–32 a.a. (amino acid) of human tau, tau was detected in the human brain and 3xTg-AD mouse brain, but not in WT and tau_{KO} mouse brains (Fig. 1a), suggesting that 113e is a human tau–specific antibody. The other tau polyclonal antibodies 111e, R134d, and 92e, reacted with both human and murine tau.

The normal human brain expresses six isoforms of tau. Their apparent molecular mass in SDS-PAGE was 48 to 67 kDa [44]. Tau proteins from AD are phosphorylated at several sites, and exhibit a higher molecular weight, 55 to 74 kDa [45]. High molecular weight tau (HMW-tau) smear in Western blots is a common feature of AD brain [7, 8, 46, 47]. Consistently, we observed HMW-tau smear in AD brain, but neither in control human nor in mouse brains (Fig. 1a). The HMW-tau aggregation was SDS- and reducing reagent–resistant. In the 113e blot, HMW-tau smear was not seen in AD, control, or mouse brains (Fig. 1a), suggesting that the N-terminus of tau may be absent or inaccessible in HMW-tau. Compared with control human brain, the level of tau in AD brain was increased by 2.5–10-fold (Fig. 1b) dependent on the antibodies under this condition (Fig. 1b). Compared with WT mouse brains, the level of tau was increased by 1.4 to 3-fold in the 3xTg-AD mouse brains, as the result of overexpression of human tau_{P301L} (Fig. 1b).

HMW-tau Smear Is Correlated with LMW-tau in AD Brain

Based on the apparent molecular weights of tau in SDS-PAGE, we divided tau into three portions, HMW-tau (> 74 kDa), medium molecular weight tau (MMW-tau, 49 to 74 kDa), and low molecular weight tau (LMW-tau, < 49 kDa) (Fig. 1a). To study alteration of tau in AD and control brains, we quantified three portions of tau by densitometry and found that almost no HMW-tau was detected in control brains, but significant amount of HMW-tau in AD brains. Little or no LMW-tau was detected in control brains, but they were detectable in AD brains (Figs. 1a and 2a). Quantification of the blots indicated that in AD brains, there were ~6% HMW-tau, 94% MMW-tau, and no LMW-tau in 113e blot; 28% HMW-tau, 49% MMW-tau, and 23% LMW-tau in 111e blot; 42% HMW-tau, 45% MMW-tau, and 13% LMW-tau in R134d blot; and 39% HMW-tau, 50% MMW-tau, and 11% LMW-tau in 92e blot (Fig. 2a). These data suggest that compared to the control brains, the proportions of HMW-tau and LMW-tau are increased, leading to reduced segment of MMW-tau, in AD brain (Fig. 2a).

To study the association between HMW-tau and LMW-tau, we performed linear correlation analysis. We found that the ratio of HMW-tau/MMW-tau was correlated with the ratio of LMW-tau/MMW-tau positively, as detected by 111e, R134d, and 92e pan-tau antibodies (Fig. 2b). Since no detectable LMW-tau in 113e blot, we were unable to analyze their correlation. These results suggest that in AD brain, the HMW-tau is correlated with LMW-tau. Thus, truncation of tau might promote the formation of HMW-tau.

HMW-tau Smear in AD brains Lacks the N-terminal Half of the Protein

We recently reported that tau in AD brain is truncated at both the N- and C-termini but predominantly at the N-terminus [47]. To extend the study and to determine tau truncation in AD and in 3xTg-AD mouse brains, we took advantage of several monoclonal antibodies to specific epitopes of tau (Fig. 3a) and analyzed tau in AD and 3xTg-AD mouse brains by Western blots developed with these antibodies (Fig. 3a).

43D targets 6–18 a.a. of human tau (Fig. 3a). We found that 43D could not detect mouse tau (Fig. 3b), confirming its specificity toward the human protein. The level of tau in AD brains was increased (Fig. 3b, c). Tau in AD brains displayed an upward mobility shift, but neither HMW-tau nor LMW-tau was seen in the 43D blot, suggesting that the N-terminus of both HMW-tau and LMW-tau was truncated in AD brain.

63B is against the second N-terminal insert (2N) of tau (Fig. 3a). A slight increase in the level of tau in AD brain was observed (Fig. 3b, c). Since 0N4R-tau_{P301L}, which cannot be detected by 63B, is overexpressed in 3xTg-AD mice, similar

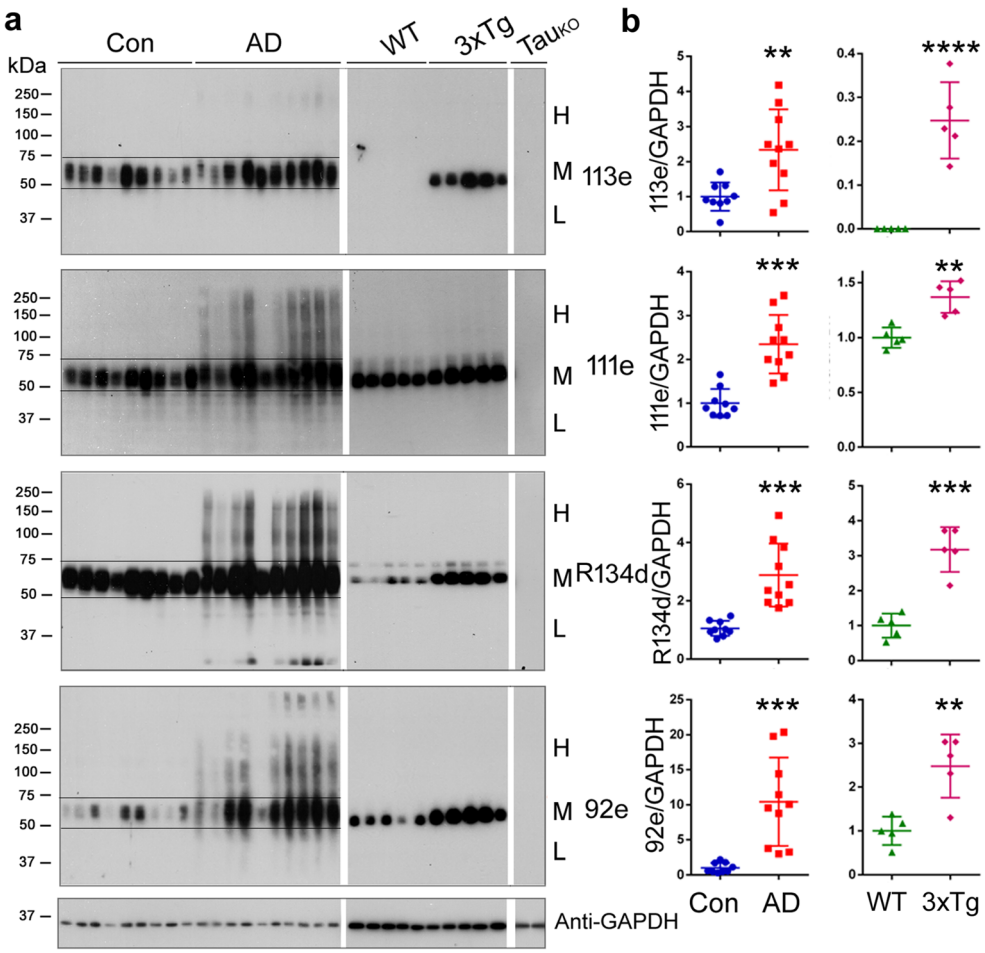

Fig. 1 Tau is increased and shows as smear in AD but not in 3xTg-AD mouse brains. Western blots of brain homogenates from control (Con) and AD cases and from wild type (WT) and 3xTg-AD mice were developed with antibodies indicated (**a**). The level of tau is shown as scattered dots with mean ± SD (**b**) and analyzed with unpaired two-tailed Student's *t* test. Two lines indicate 74 kDa and 49 kDa respectively. H, high molecular weight tau; M, middle molecular weight tau; L, low molecular weight tau. $^{**}p < 0.01$, $^{***}p < 0.001$, $^{****}p < 0.0001$

levels of tau (mouse tau) were observed in WT and 3xTg-AD mouse brains by using 63B, as expected (Fig. 3b, c). No tau, but IgG heavy chain (HC), was detected in tau_{KO} mouse brains (Fig. 3b). In AD brains, 63B stained some LMW-tau but not HMW-tau (Fig. 3b), suggesting that the first 100 a.a. residues probably are absent in the SDS/reducing reagent-resistant HMW-tau. There was no detectable LMW-tau in either WT or 3xTg-AD mouse brains by using 63B (Fig. 3b).

The epitopes of HT7 and 39E10 are a.a.159–163 and a.a. 189–195 of human tau, respectively (Fig. 3a). The level of tau was found to be increased in HT7 blot but not in 39E10 blot in AD brain (Fig. 3b). HT7 was reported to be a human specific antibody [48, 49], but we found weak signal in WT mouse brain (Fig. 3b). In addition, we observed ~ 75-kDa bands in HT7-blots in WT, 3xTg-AD, and tau_{KO} mouse brains (Fig. 3b), suggesting the non-specific immunoreaction to these mouse brain proteins. The level of tau in 3xTg-AD mice was increased in 39E10-blot (Fig. 3b, c). Similar to 43D and 63B, HMW-tau in AD brains very weakly immunoreacted with either HT7 or 39E10 (Fig. 3b). Thus, majority of HMW-tau in AD brain did not contain the first 195 a.a.. Some LMW-tau was detectable in both control and AD brains, but not in mouse brains by these two antibodies (Fig. 3b).

Tau5 targets tau at a.a. 210–230 (Fig. 3a). The level of tau was increased in AD and in 3xTg-AD mouse brains compared with their corresponding controls (Fig. 3b, c). No tau was detected by tau5 in Tau_{KO} mouse brain (Fig. 3b), confirming its specificity toward tau. We observed HMW-tau and LMW-tau in tau5 blot in AD brains (Fig. 3b), indicating that the HWM smears in AD brain contain tau5 epitope. Consistently, we did not detect HMW-tau and LMW-tau in either WT or 3xTg-AD mouse brains (Fig. 3b) under this conditions.

77G7 targets the microtubule-binding repeats of tau (Fig. 3a). We found that 77G7 strongly reacted with all HMW-tau, MMW-tau, and LMW-tau (Fig. 3b), leading to a marked increase in the 77G7-tau level in AD brain (Fig. 3c). 77G7 also reacted with recombinant tau (Data not shown) and tau in WT mouse brain. These results suggest a high affinity of 77G7 to AD tau. The level of 77G7-tau was increased, but no HMW-tau smear or LMW-tau was detected by 77G7 in 3xTg-AD mouse brain (Fig. 3b, c). The specificity of 77G7 was verified by using tau_{KO} mouse brain with only a weak band of IgG heavy chain (Fig. 3b).

Tau46, an antibody against the C-terminal portion of tau (Fig. 3a), also reacted with HMW-tau, MMW-tau, and LMW-tau (Fig. 3b). The levels of tau in AD and 3xTg-AD mouse

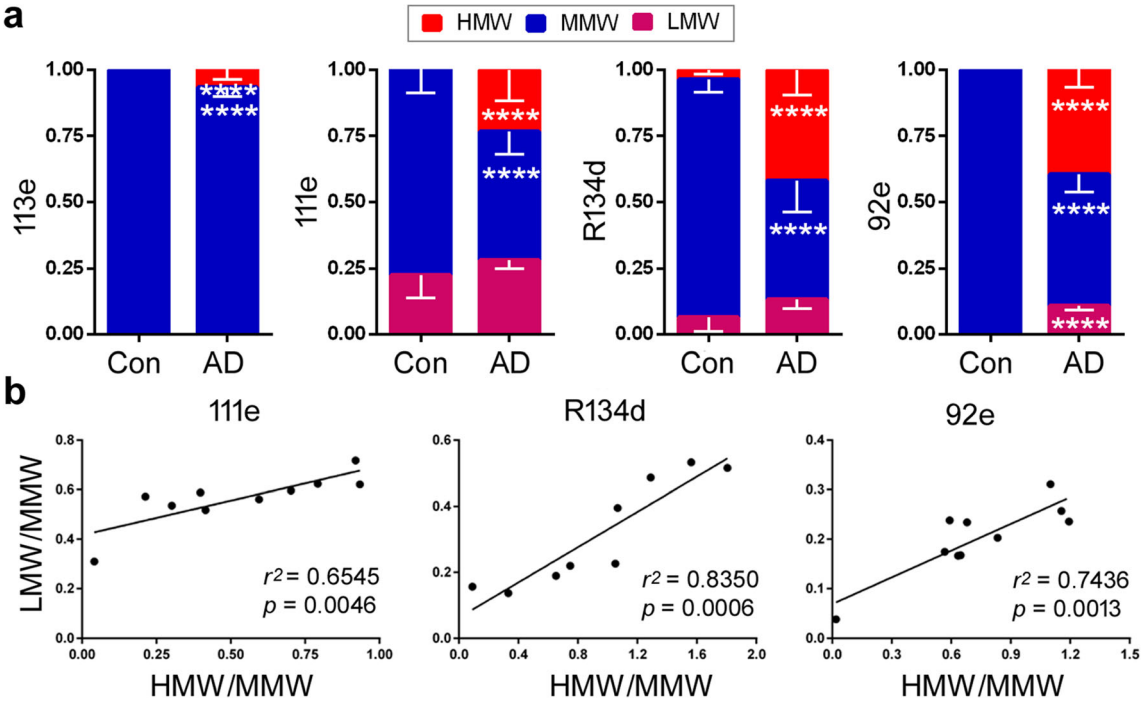

Fig. 2 HMW-tau smear and LMW-truncated tau are increased and correlated positively in AD brain. **a** The HMW-tau, MMW-tau, and LMW-tau in Fig. 1a were quantified by densitometry and analyzed by two-way ANOVA followed by Sidak's multiple comparisons test. The total tau level was defined as 1. The data are presented as mean ± SD; ****$p < 0.0001$. **b** The ratios of LMW-tau/MMW-tau are plotted against the ratio of HMW-tau/MMW-tau. The Pearson correlation analysis was performed

brains were increased compared with their corresponding controls (Fig. 3a, b). Same as above antibodies, no HMW-tau smears or LMW-tau were seen in 3xTg-mouse brains with Tau46 (Fig. 3b).

Taken together, these results suggest that the SDS/reducing reagent-resistant HMW-tau smear is present only in AD brain, but not in control human, WT, or aged 3xTg-AD mouse brains. The N-terminal half of tau may be truncated in the HMW-tau smear in AD brain. The truncated LMW-tau is increased in AD brain. The level of tau is increased in AD brain and in 3xTg-AD mouse brain.

Antibody Against the Microtubule-Binding Repeats Detects the Highest Level of HMW-tau Smear and Truncated LMW-tau in AD brains

To study the relationship of HMW-tau with the truncation of tau in AD brains, we analyzed the relative levels of HMW-tau, MMW-tau, and LMW-tau detected above (Fig. 3b). We found that consistent to data from Western blots developed with polyclonal antibodies (shown in Fig. 2), no or trace amount of HMW-tau in control brains was detected by these monoclonal antibodies (Figs. 3b and 4a). Compared with control brains, LMW-tau and/or HMW-tau were increased in AD brains in Western blots developed by some monoclonal antibodies (Figs. 3b and 4a), leading to a decrease in the proportion of MMW-tau (Fig. 4a).

In AD brains, no or very little of HMW-tau was found in 43D, 63B, HT7, and 39E10 blots, suggesting that the N-terminal half of tau is not present in the HMW-tau smear. We also found that 0%, 37%, 12%, and 17% LMW-tau in AD brain in 43D, 63B, HT7, and 39E10 blots, respectively (Fig. 4a). Different from the N-terminal antibodies, 32% HMW-tau, 56% MMW-tau, and 12% LMW-tau were detected by using tau5, 40% HMW-tau, 19% MMW-tau, and 41% LMW-tau by 77G7 blot and 56% HMW-tau, 37% MWW-tau, and 7% LMW-tau by tau46 blot in AD brain (Fig. 4a).

Then we compared the ratio of HMW-tau/MMW-tau or LMW-tau/MMW-tau in AD brains detected by these monoclonal antibodies. We found that antibody 77G7 detected the highest levels of both HMW-tau/MMW-tau and LMW-tau/MMW-tau (Fig. 4b, c). These results suggest that the pathological HMW-tau and LMW-tau both may lack the N-terminal half and the C-terminal end of tau molecules.

Tau Phosphorylation Is Robustly Increased in AD, but Only Slightly Increased in 3xTg-AD Mouse Brains

To compare the phosphorylation levels of tau between AD brains and 3xTg-AD mouse brains, we analyzed tau phosphorylation by Western blots developed with site-specific and phosphorylation-dependent tau antibodies (Fig. 5). We found that phosphorylation of tau was increased robustly at all sites detected, including Ser199, Ser202/Thr205 (AT8

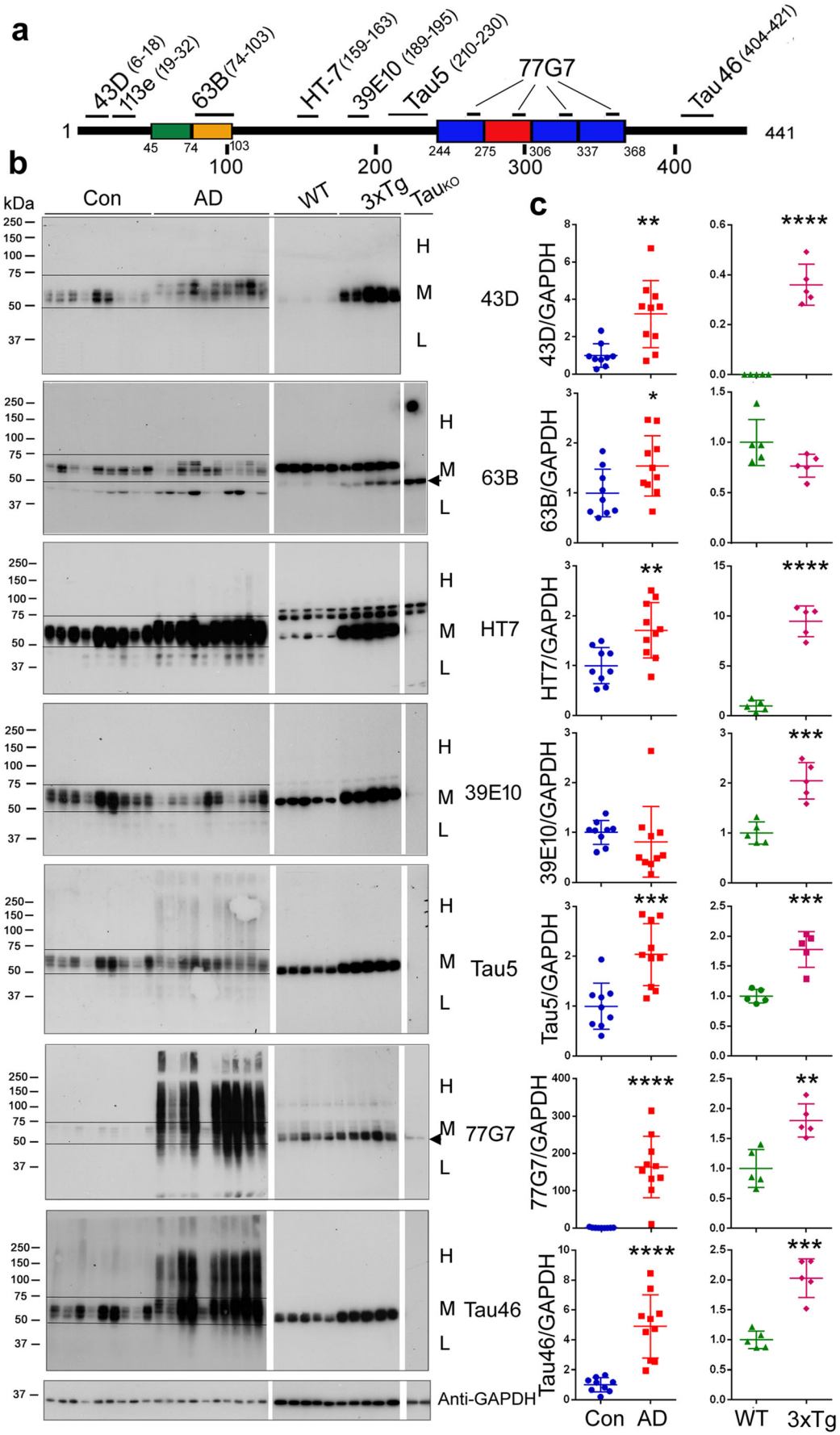
a
43D (6-18)
113e (19-32)
63B(74-103)
HT-7(159-163)
39E10 (189-195)
Tau5 (210-230)
77G7
Tau46(404-421)
1
441
45
74
103
244
275
306
337
368
100
200
300
400
b
kDa
Con
AD
WT
3xTg
TauKO
250
150
100
75
50
37
H
M
L
43D
63B
HT7
39E10
Tau5
77G7
Tau46
Anti-GAPDH
c
43D/GAPDH
63B/GAPDH
HT7/GAPDH
39E10/GAPDH
Tau5/GAPDH
77G7/GAPDH
Tau46/GAPDH
**
*
****
***
Con
AD
WT
3xTg

◀ **Fig. 3** HMW-tau smear in AD brains lacks the N-terminus. **a** Schematic showing the position of epitopes of tau antibodies used in the present study. **b**, **c** Western blots of brain homogenates were developed with the indicated tau antibodies (**b**). Two lines indicate 74 kDa and 49 kDa respectively. The levels of total tau level are presented as scattered graphs with mean ± SD and analyzed with unpaired two-tailed Student's *t* test for all blots except Mann-Whitney *U* test for blots of 39E10 and 77G7 for human samples. *$p < 0.05$, **$p < 0.01$, ***$p < 0.001$, ****, $p < 0.0001$. Arrowhead, IgG heavy chain; H, HMW-tau; M, MMW-tau; L, LMW-tau

sites), Thr205, Thr212, Ser214, Thr217, Ser262, Ser396/Ser404 (PHF-1 sites), and Ser422, in AD brains (Fig. 5a, b). HMW-tau, MMW-tau, and LMW-tau were all immunorecognized by these phospho-tau antibodies (Fig. 5a). We found some non-specific signals in blots developed with anti-pSer262 and anti-pSer422 (Fig. 5a).

We did not find HMW-tau smear or LMW-tau in 3xTg-AD mouse brains in any blots developed with these phospho-tau antibodies (Fig. 5a). The phosphorylated tau in 3xTg-AD mouse brains was increased slightly at all detected sites (Fig. 5a). However, the net phosphorylation level of tau after being normalized with Tau5 was not increased at Ser199, Ser214, Ser396/404, or Ser422, while slightly increased at AT8 sites, Thr205, Thr212, Thr217, and Ser262. Thus, unlike robust abnormal hyperphosphorylation of tau in AD brain, tau phosphorylation was slightly increased site-specifically in 3xTg-AD mice. In addition, we observed non-specific reactions in the blots developed with AT8, anti-pT212, anti-pS214, anti-pT217, anti-pS262, and anti-pS422 (see the bands in Tau_{KO} samples) (Fig. 5).

Oligomeric Tau Aggregates in AD Brains Differ from Those in 3xTg-AD Mouse Brains

To compare tau pathology in AD brains and in 3xTg-AD mouse brains, we immunostained the AD and 3xTg-AD mouse (22-month-old) brain tissue sections with AT8 (pSer202/Thr205-tau) antibody. The phospho-tau immunostaining of AD brain sections with AT8 revealed filamentous inclusions not only in the somatodendritic compartment of neurons but also as dystrophic neurites (Fig. 6a). In contrary to compact filamentous inclusions seen in AD brain, tau pathology in the brains of the 3xTg-AD mouse model predominantly showed a truffle-like morphology even when the mice were as aged as 22 months old (Fig. 6a). These observations suggest a marked

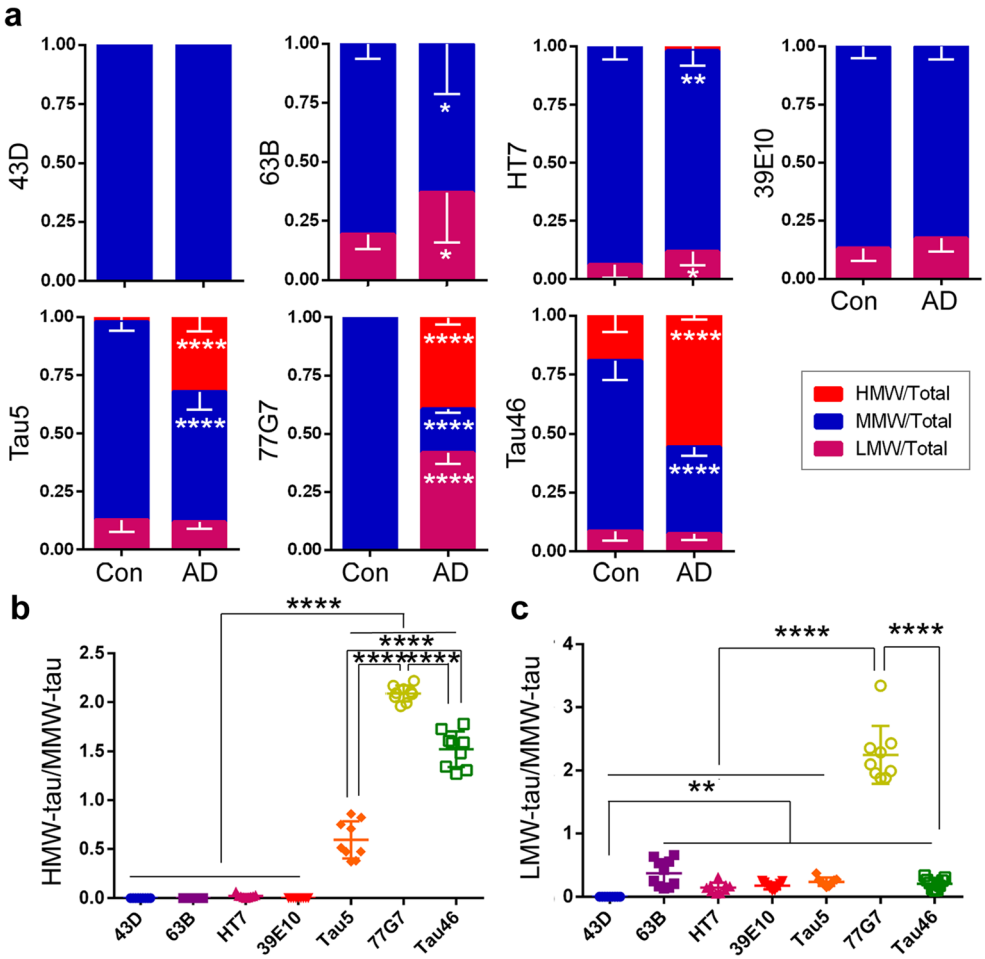

Fig. 4 Antibodies against various epitopes of tau detect different levels of HMW-tau, MMW-tau, and LMW-tau in human brains. **a** Proportions of HMW-tau, MMW-tau, and LMW-tau in AD and control brains determined by Western blots in Fig. 3b were analyzed and presented as mean ± SD. **b**, **c** The ratios of HMW-tau/MMW-tau and LMW-tau/MMW-tau in AD brains were analyzed and are presented as scattered graph (mean ± SD) and analyzed by one-way ANOVA followed by Tukey's multiple comparisons test. *$p < 0.05$, **$p < 0.01$, ****$p < 0.0001$

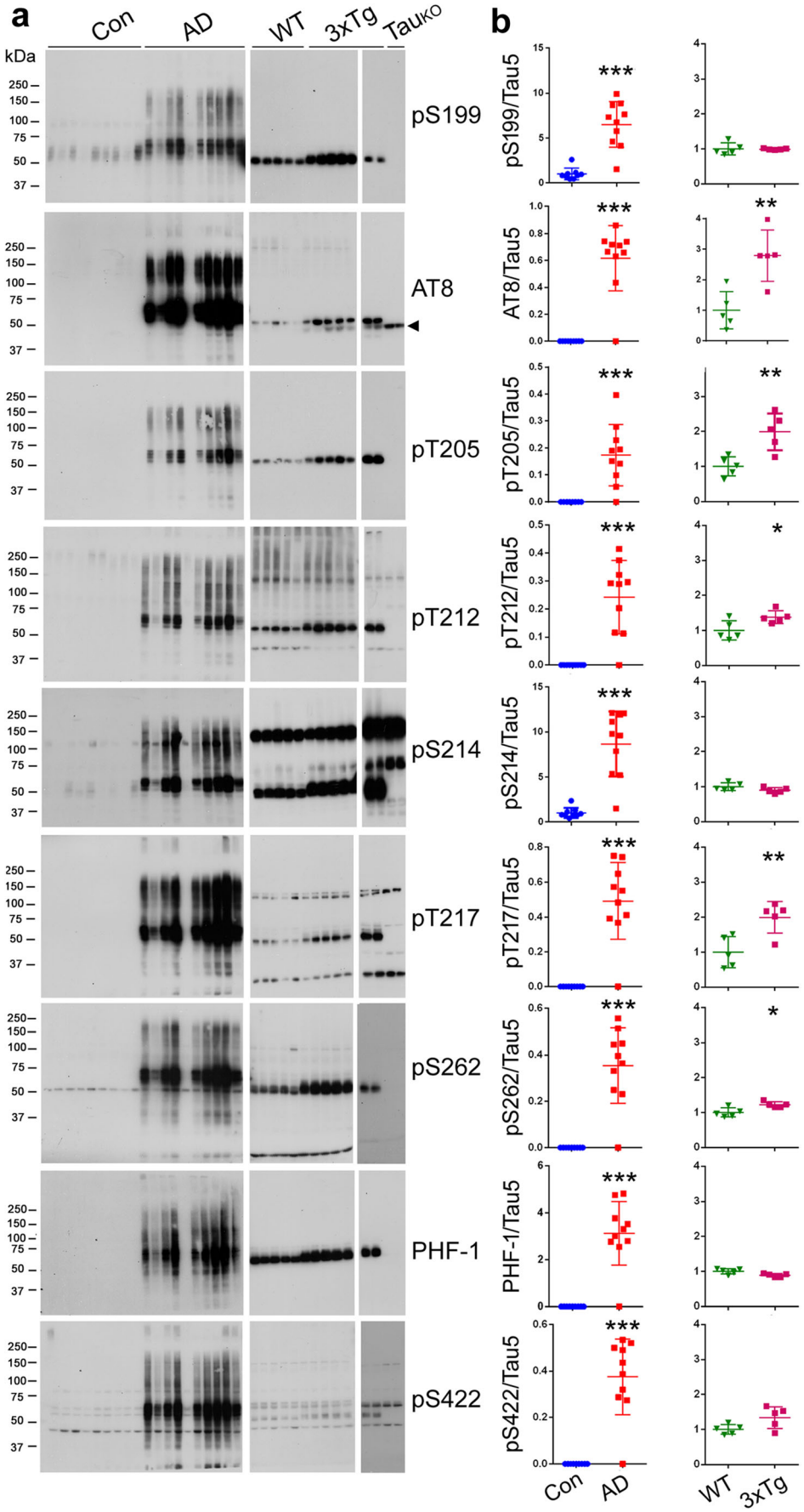
a
Con
AD
WT
3xTg
TauKO
kDa
250
150
100
75
50
37
pS199
AT8
pT205
pT212
pS214
pT217
pS262
PHF-1
pS422
b
pS199/Tau5
AT8/Tau5
pT205/Tau5
pT212/Tau5
pS214/Tau5
pT217/Tau5
pS262/Tau5
PHF-1/Tau5
pS422/Tau5
***
**
*
Con
AD
WT
3xTg

◀ **Fig. 5** Tau is abnormally hyperphosphorylated in AD brains and slightly hyperphosphorylated in 3xTg-AD mouse brains. Phosphorylation of tau in brain homogenates was analyzed by Western blots developed with site-specific and phosphorylation-dependent tau antibodies as indicated (**a**) and is presented as mean ± SD (**b**) and analyzed with Mann-Whitney *U* test. *$p < 0.05$, **$p < 0.01$, ***$p < 0.001$

difference in the assembly of neuronal tau aggregates between the 3xTg-AD mouse brains and AD brains.

We previously found that hyperphosphorylated and oligomeric tau isolated from AD brain captures normal tau in vitro [11] and templates tau aggregation in vivo [25]. We thus isolated oligomeric tau from AD and 22-month-old 3xTg-AD mouse brains as described previously [9, 25] and analyzed them by Western blots. We found that Oligo-tau from 3xTg-AD and AD brains were immunoreactive with polyclonal tau antibodies, 111e, R134d, and 92e (Fig. 6b). As seen in AD brain homogenates, we observed HMW-tau in the Oligo-tau

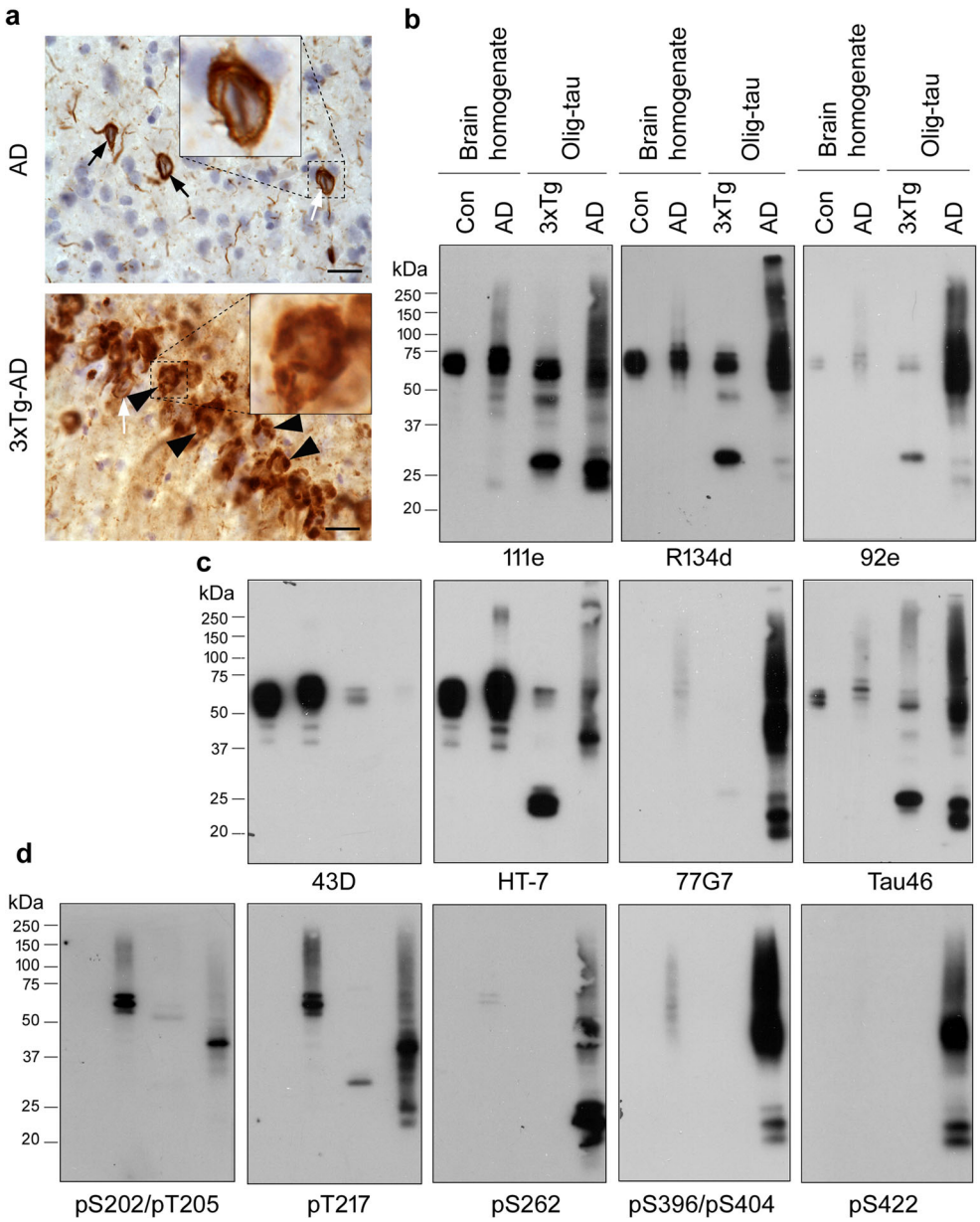

Fig. 6 Oligomeric tau from AD brains, but not from 3xTg-AD mouse brains, is hyperphosphorylated and aggregated to high molecular weight smear in Western blots. **a** Immunostaining for pSer202/Thr205-tau with antibody AT8 reveals distinct morphology of neuronal tau inclusions in the aged 3xTg-AD mouse brains compared to that in AD brains. In contrast to filamentous tau inclusions (dark arrows) in the somatodendritic compartment of neurons in AD brain, majority of neuronal tau inclusions in brains of 22-month-old 3xTg-AD mice exhibit truffle-like morphology (arrowheads) with a small subset of neurons showing less compact filamentous inclusions (white arrows). Scale bars represent 20 μm. **b**–**d** Western blots of the homogenates from control and AD brains and Oligo-tau isolated from AD and 3xTg-AD mouse brains were developed with polyclonal antibodies (**b**), monoclonal antibodies (**c**), and site-specific and phosphorylation-dependent antibodies indicated (**d**)

preparations from AD brains, but not from 3xTg-AD mouse brains except with Tau46 (Fig. 6b–d). Different from 3xTg-AD mice, Oligo-tau from AD was almost undetectable by 43D (Fig. 6c), suggesting that Oligo-tau lacks the N-terminus, which is consistent with our conclusion that HMW-tau was truncated at the N-terminus in AD brain based on our results showed alone in Figs. 1a and 3b.

Oligo-tau from both AD and 3xTg-AD mouse brains was detectable with HT7 and Tau46 (Fig. 6c), but Oligo-tau from 3xTg-AD mouse brains was very weakly detected by 77G7 (Fig. 6c). HMW-tau smears of Oligo-tau from AD brain were observed in HT7, 77G7, and Tau46 blots, but those from 3xTg-AD mouse brains were only seen in the blot developed with Tau46 (Fig. 6c). Truncated LMW-tau in Oligo-tau from AD brains was detected by 111e, R134d, 92e, HT7, 77G7, and Tau46, whereas that from 3xTg-AD mouse brains was showed in the blots of 111e, R134d, 92e, HT7, and Tau46.

Western blots of Oligo-tau preparations by using phosphorylation-dependent tau antibodies showed that Oligo-tau from AD brains, but not from 3xTg-AD mouse brains, was hyperphosphorylated at Ser202/Thr205 (AT8), Thr217, Ser262, Ser396/404 (PHF-1), and Ser422 (Fig. 6d). The HMW-smear and truncated LMW-tau of Oligo-tau from AD brain also were hyperphosphorylated at these sites (Fig. 6d). Taken together, these results reveal different pathological alterations of Oligo-tau between AD brains and 3xTg-AD mouse brains. Oligo-tau from AD brain is truncated at the N-terminus, hyperphosphorylated, and forms HMW-tau smear, which resists to denaturing condition, reducing and SDS.

Oligo-tau from AD Brains Has More Potent Prion-Like Activity Than That from 3xTg-AD Mouse Brains

To compare the prion-like activity of Oligo-tau from AD brains with that from 3xTg-AD mouse brains, we dotted the same amount of Oligo-tau, as determined by immuno-dot blots developed with the mixture of pan-tau antibodies R134 and 92e, with serial dilutions on nitrocellulose membrane (Fig. 7a). After blocking, the membrane was incubated with the extract of HEK-293FT/HA-tau$_{151–391}$. Tau$_{151–391}$ represents the proteinase-K resistant fragment of PHF [50, 51], which is prone to aggregation. The captured HA-tau$_{151–391}$ was then detected with polyclonal anti-HA followed with HRP-anti-rabbit-IgG. We found that Oligo-tau from AD brains and from 3xTg-AD mouse brains both captured tau$_{151–391}$ dose dependently (Fig. 7b, c), but Oligo-tau from AD brain showed much higher ability to capture tau than that from 3xTg-AD mouse brains, suggesting that Oligo-tau from AD brains is more potent in the prion-like activity than that from 3xTg-AD mouse brains.

Tau aggregates are able to seed tau aggregation [27, 28]. To determine the seeding activity in cultured cells of the two Oligo-taus, we overexpressed HA-tau$_{151–391}$ in HeLa cells and added Oligo-tau into the cultures for 42 h. We then immunostained the cells with anti-HA. We found that without adding Oligo-tau, a few cells showed tau aggregates (Fig. 7d, e). However, a large number of cells with aggregates was seen after adding Oligo-tau from AD brains (Fig. 7d, e). However, under this condition, we did not observe significant tau aggregates in cells treated with Oligo-tau from 3xTg-AD mouse brain (Fig. 7d, e). These results indicate that Oligo-tau from AD brains, but not from 3xTg-AD mouse brains, seeds tau aggregation in cultured cells.

Discussion

In the present study, we determined the pathological alterations of tau in AD and 3xTg-AD mouse brains and analyzed the prion-like properties of Oligo-tau isolated from these brains. We found that tau exhibited high molecular weight smears in AD brains, but not in 3xTg-AD mouse brains. The high molecular weight smear tau lacked the N-terminal portion and was hyperphosphorylated at multiple sites. Significant level of low molecular weight truncated tau was also seen in AD brain, but not in 3xTg-AD mouse brains. We found the filamentous tau staining with AT8 in AD brains and truffle-like structures in 3xTg-AD mouse brains. Furthermore, the oligomeric tau isolated from AD brains, compared to that from 3xTg-AD mouse brains, showed much strong prion-like activity, including capture of tau in vitro and templating tau into aggregates in cultured cells. Thus, very limited pathological alterations of tau were observed in 3xTg-AD mouse brains in terms of hyperphosphorylation, truncation, aggregation, and prion-like properties.

Oligomers and PHF-tau are known to present as a smear in Western blots [7–9, 46]. In the present study, we found that the high molecular weight smears were present specifically in AD brains, but not in control human brains in Western blots, suggesting the HMW-tau is SDS- and reducing condition–resistant. In addition to HMW-smear tau, LMW-truncated tau was increased in AD brain, which correlated positively with the HMW-tau. The HMW-tau did not react with a pool of antibodies against the N-terminal portion of tau, including 43D, 113e, 63D, HT7, and 39E10, indicating that the HMW-tau might not contain the first 200 amino acids and is the aggregates of the C-terminal half of tau. From the N- to C-termini, the levels HMW-tau and LMW-tau in AD brain were found to be increased gradually and peaked at the microtubule-binding repeat region of tau. The HMW-tau smear and LMW-truncated tau were not detectable in wild type or 3xTg-AD mouse brains, suggesting no or minimal

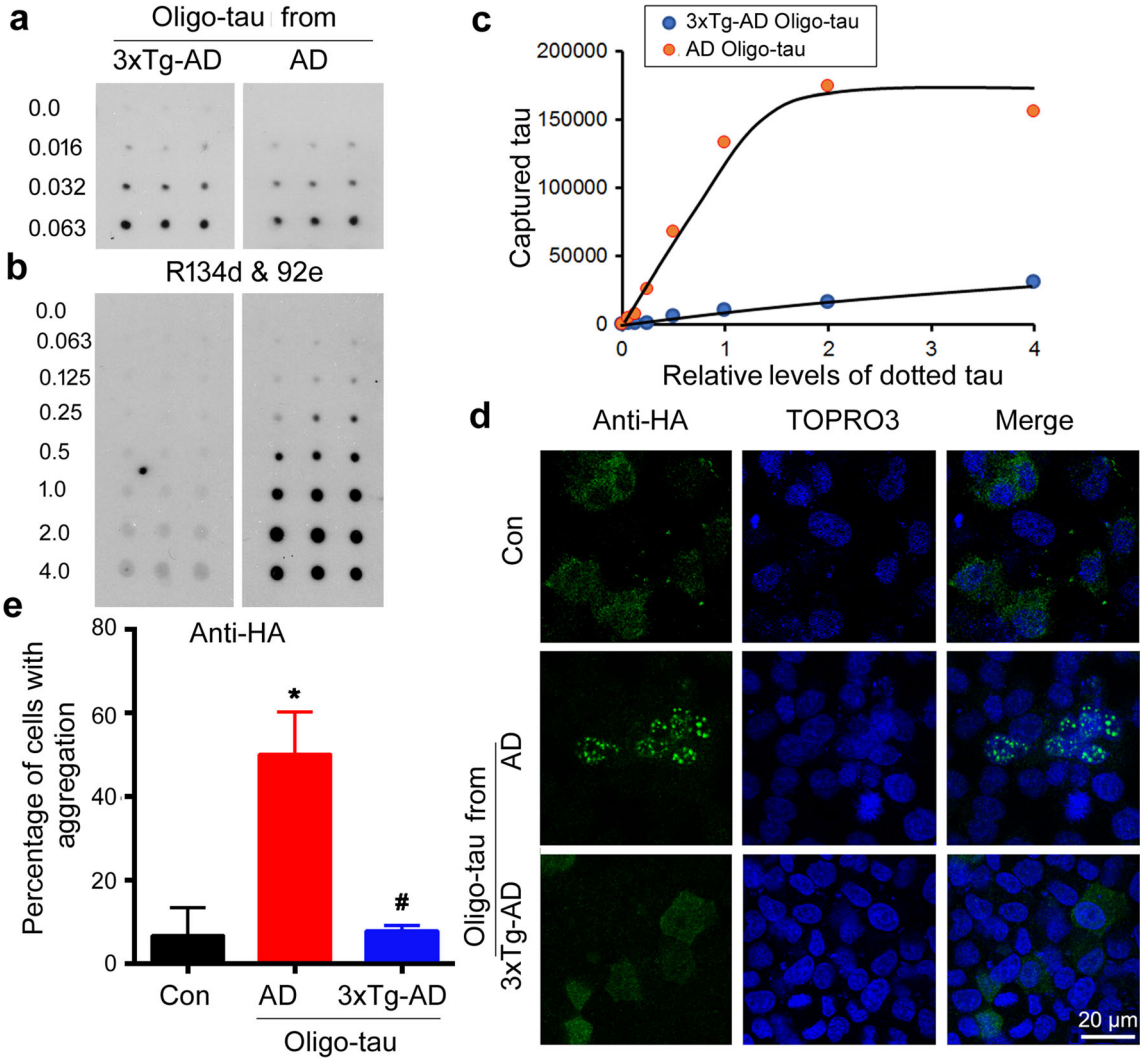

Fig. 7 Oligomeric tau from AD brains shows far stronger activity to capture tau and to seed tau aggregation than that from 3xTg-AD mouse brains. **a**–**c** Levels of tau in Oligo-tau preparations from AD and 3xTg-AD mouse brains were analyzed by immuno-dot blots developed with the mixture of R134d and 92e (**a**). The same amount of tau of Oligo-tau from AD and 3xTg-AD mouse brains was dotted with different dilutions on nitrocellulose membrane and overlaid with HA-tau$_{151–391}$-cell lysate. The captured HA-tau$_{151–391}$ by Oligo-tau was analyzed by anti-HA (**b**) and plotted against tau level in Oligo-tau (**c**). **d**, **e** HA-tau$_{151–391}$ was expressed in HeLa cells. The cells were treated with Oligo-tau from AD or 3xTg-AD mouse brains and immunostained with anti-HA. TO-PRO3 was used for staining nuclei. The HA-tau expressing cells with aggregates were counted and data are presented as mean ± SD and analyzed with one-way ANOVA. *$p < 0.05$ vs. control, $^{\#}p < 0.05$ vs. AD-Oligo-tau

increase in truncation and AD-type tau aggregation in 3xTg-AD mouse brains.

Tau in AD brain was abnormally hyperphosphorylated at multiple sites. HMW-smear tau was also phosphorylated at all sites detected in the present study. In 3xTg-AD mouse brain, human tau$_{P301L}$ was overexpressed. However, the level of phosphorylated tau in 3xTg-AD mouse was not or only slightly increased at specific sites. Furthermore, no phosphorylated HMW-tau smears were found in 3xTg-AD mouse brains. Thus, compared with robust abnormal phosphorylation in AD brain, tau was minimally phosphorylated in 3xTg-AD mouse brains.

Previous studies demonstrated that hyperphosphorylation of tau changes its conformation and promotes its aggregation. During tangle maturation, tau is truncated at the N- and C-termini to form compressed filamentous structure [52, 53]. We found in the present study that tau tangles in AD brains appeared as filamentous staining by AT8, while they displayed the truffle-like staining in 3xTg-AD mouse brains. No LMW-truncated and HMW-tau smear taus were detected in 3xTg-AD mice, suggesting that truncation may be critical for the formation of filamentous tangles.

It was reported two decades ago that hyperphosphorylated and oligomeric tau isolated from AD brain captures and templates normal tau to form aggregates in vitro [11], which might be the molecular basis of the propagation of tau pathology in AD brain. In the present study, we used tau$_{151–391}$ for the sequestration assay and seeding to aggregation in cultured cells. Tau$_{151–391}$

was identified as the core of PHFs and is prone to aggregation [50, 51]. Transgenic rats expressing $tau_{151–391}$ develop neurofibrillary pathology and also display hyperphosphorylation and production of HMW-tau species [54]. We found here that Oligo-tau from AD brain was hyperphosphorylated and truncated and presented as HMW-tau smears in Western blots. However, Oligo-tau from 3xTg-AD mouse brain did not show as HMW-tau smear, suggesting 3xTg-AD Oligo-tau is not SDS- and reducing agent –resistant. Moreover, different from hyperphosphorylation of AD Oligo-tau, 3xTg-AD Oligo-tau was markedly less hyperphosphorylated, but may contain truncated fragments of tau. AD Oligo-tau captured normal tau, but 3xTg-AD Oligo-tau failed to do so. Similarly, AD Oligo-tau, but not 3xTg-AD Oligo-tau, seeded tau to form aggregates in cultured cells. Thus, hyperphosphorylation and/or SDS- and reducing condition–resistant aggregation may be responsible for Oligo-tau seeding activity.

In addition to determining the pathological changes in AD and 3xTg-AD mouse brains, specificity of tau antibodies was analyzed. Polyclonal antibodies 111e, R134d, and 92e immunoreacted with tau in the human brains and in WT and 3xTg-AD mouse brains, but did not react with that in tau_{KO} mouse brains, suggesting that they are specific anti-tau antibodies. 113e did not react with WT mouse brain, confirming that it is human-specific.

In case of monoclonal tau antibody 43D, no immunosignal of mouse tau was detected, suggesting it is a human tau specific antibody. 63B, 39E10, Tau5, 77G7, and Tau46 immunoreacted with tau in the human and mouse brains, but not in tau_{KO} mouse brains, suggesting they are specific toward tau. HT7 is a human tau–specific antibody [48]. However, we found it also weakly reacted with mouse tau. In addition, there was non-specific reaction in mouse brain in HT7 blots. It is noteworthy to mention that IgG heavy chain and/or light chain in mouse brain can be immunorecognized by some mouse monoclonal antibodies.

Most of the site-specific and phosphorylation-dependent tau antibodies are polyclonal antibodies from rabbit. No immunoreactivity was observed in the blots of tau_{KO} mice developed with anti-pSer199 and anti-pThr205, suggesting that these two antibodies are highly specific to tau. The antibodies anti-pThr212, anti-pSer214, anti-pThr217, anti-pSer262, and anti-pSer422 showed other immunoreactive bands besides tau in Western blots, indicating their cross-reactivity with other proteins in the human and/or mouse brains. Monoclonal PHF-1 did not have any immunoreactivity in tau_{KO} mouse brain, indicating its high specificity.

To summarize, we found that the pathological changes of tau in 3xTg-AD mouse brains differ from that of AD brains due to lack of the N-terminal truncation, minimal HMW-tau smears resulting from aggregation, and only slight hyperphosphorylation, which may collectively result in much weaker potency in the prion-like activities.

Funding Information This work was supported in part by funds from Nantong University, New York State Office for People Developmental Disabilities, and the Neural Regeneration Co-innovation Center of Jiangsu Province and by grants from US Alzheimer's Association (DSAD-15-363172, 2016-NIRG-397030) and Postgraduate Research and Practice Innovation Program of Jiangsu Province (KYCX18_2413).

Compliance with Ethical Standards

Conflict of Interest The authors declare that they have no conflict of interest.

Publisher's Note Springer Nature remains neutral with regard to jurisdictional claims in published maps and institutional affiliations.

References

1. Iqbal KGrundke-Iqbal I (2010) Alzheimer's disease, a multifactorial disorder seeking multitherapies. Alzheimers Dement 6(5):420–424
2. Gong CX, Liu F, Iqbal K (2018) Multifactorial hypothesis and multi-targets for Alzheimer's disease. J Alzheimers Dis 64(s1): S107–S117
3. Tomlinson BE, Blessed G, Roth M (1970) Observations on the brains of demented old people. J Neurol Sci 11(3):205–242
4. Alafuzoff I, Iqbal K, Friden H, Adolfsson R, Winblad B (1987) Histopathological criteria for progressive dementia disorders: clinical-pathological correlation and classification by multivariate data analysis. Acta Neuropathol 74(3):209–225
5. Arriagada PV, Growdon JH, Hedley-Whyte ET, Hyman BT (1992) Neurofibrillary tangles but not senile plaques parallel duration and severity of Alzheimer's disease. Neurology 42(3 Pt 1):631–639
6. Quiroz YT, Sperling RA, Norton DJ, Baena A, Arboleda-Velasquez JF, Cosio D, Schultz A, Lapoint M et al (2018) Association between amyloid and tau accumulation in young adults with autosomal dominant Alzheimer disease. JAMA Neurol 75:548–556
7. Grundke-Iqbal I, Iqbal K, Quinlan M, Tung YC, Zaidi MS, Wisniewski HM (1986) Microtubule-associated protein tau. A component of Alzheimer paired helical filaments. J Biol Chem 261(13):6084–6089
8. Grundke-Iqbal I, Iqbal K, Tung YC, Quinlan M, Wisniewski HM, Binder LI (1986) Abnormal phosphorylation of the microtubule-associated protein tau (tau) in Alzheimer cytoskeletal pathology. Proc Natl Acad Sci U S A 83(13):4913–4917
9. Kopke E, Tung YC, Shaikh S, Alonso AC, Iqbal K, Grundke-Iqbal I (1993) Microtubule-associated protein tau. Abnormal phosphorylation of a non-paired helical filament pool in Alzheimer disease. J Biol Chem 268(32):24374–24384
10. Alonso AC, Zaidi T, Grundke-Iqbal I, Iqbal K (1994) Role of abnormally phosphorylated tau in the breakdown of microtubules in Alzheimer disease. Proc Natl Acad Sci U S A 91(12):5562–5566
11. Alonso AC, Grundke-Iqbal I, Iqbal K (1996) Alzheimer's disease hyperphosphorylated tau sequesters normal tau into tangles of filaments and disassembles microtubules. Nat Med 2(7):783–787
12. Lindwall GCole RD (1984) Phosphorylation affects the ability of tau protein to promote microtubule assembly. J Biol Chem 259(8): 5301–5305
13. Alonso A, Zaidi T, Novak M, Grundke-Iqbal I, Iqbal K (2001) Hyperphosphorylation induces self-assembly of tau into tangles of paired helical filaments/straight filaments. Proc Natl Acad Sci U S A 98(12):6923–6928

14. Kovacech B, Novak M (2010) Tau truncation is a productive post-translational modification of neurofibrillary degeneration in Alzheimer's disease. Curr Alzheimer Res 7(8):708–716
15. Holmes BBDiamond MI (2014) Prion-like properties of tau protein: the importance of extracellular Tau as a therapeutic target. J Biol Chem 289(29):19855–19861
16. Margittai M, Langen R (2004) Template-assisted filament growth by parallel stacking of tau. Proc Natl Acad Sci U S A 101(28): 10278–10283
17. Weismiller HA, Murphy R, Wei G, Ma B, Nussinov R, Margittai M (2018) Structural disorder in four-repeat Tau fibrils reveals a new mechanism for barriers to cross-seeding of Tau isoforms. J Biol Chem 293(45):17336–17348
18. Braak H, Braak E (1991) Neuropathological stageing of Alzheimer-related changes. Acta Neuropathol 82(4):239–259
19. Braak H, Del Tredici K (2011) Alzheimer's pathogenesis: is there neuron-to-neuron propagation? Acta Neuropathol 121(5):589–595
20. Clavaguera F, Bolmont T, Crowther RA, Abramowski D, Frank S, Probst A, Fraser G, Stalder AK et al (2009) Transmission and spreading of tauopathy in transgenic mouse brain. Nat Cell Biol 11(7):909–913
21. Ahmed Z, Cooper J, Murray TK, Garn K, McNaughton E, Clarke H, Parhizkar S, Ward MA et al (2014) A novel in vivo model of tau propagation with rapid and progressive neurofibrillary tangle pathology: the pattern of spread is determined by connectivity, not proximity. Acta Neuropathol 127(5):667–683
22. Takeda S, Wegmann S, Cho H, DeVos SL, Commins C, Roe AD, Nicholls SB, Carlson GA et al (2015) Neuronal uptake and propagation of a rare phosphorylated high-molecular-weight tau derived from Alzheimer's disease brain. Nat Commun 6:8490
23. Clavaguera F, Akatsu H, Fraser G, Crowther RA, Frank S, Hench J, Probst A, Winkler DT et al (2013) Brain homogenates from human tauopathies induce tau inclusions in mouse brain. Proc Natl Acad Sci U S A 110(23):9535–9540
24. Boluda S, Iba M, Zhang B, Raible KM, Lee VM, Trojanowski JQ (2015) Differential induction and spread of tau pathology in young PS19 tau transgenic mice following intracerebral injections of pathological tau from Alzheimer's disease or corticobasal degeneration brains. Acta Neuropathol 129(2):221–237
25. Hu W, Zhang X, Tung YC, Xie S, Liu F, Iqbal K (2016) Hyperphosphorylation determines both the spread and the morphology of tau pathology. Alzheimers Dement 12(10):1066–1077
26. Dai CL, Hu W, Tung YC, Liu F, Gong CX, Iqbal K (2018) Tau passive immunization blocks seeding and spread of Alzheimer hyperphosphorylated Tau-induced pathology in 3xTg-AD mice. Alzheimers Res Ther 10(1):13
27. Frost B, Jacks RL, Diamond MI (2009) Propagation of tau misfolding from the outside to the inside of a cell. J Biol Chem 284(19):12845–12852
28. Sanders DW, Kaufman SK, DeVos SL, Sharma AM, Mirbaha H, Li A, Barker SJ, Foley AC et al (2014) Distinct tau prion strains propagate in cells and mice and define different tauopathies. Neuron 82(6):1271–1288
29. Clavaguera F, Lavenir I, Falcon B, Frank S, Goedert M, Tolnay M (2013) "Prion-like" templated misfolding in tauopathies. Brain Pathol 23(3):342–349
30. Oddo S, Caccamo A, Shepherd JD, Murphy MP, Golde TE, Kayed R, Metherate R, Mattson MP et al (2003) Triple-transgenic model of Alzheimer's disease with plaques and tangles: intracellular Abeta and synaptic dysfunction. Neuron 39(3):409–421
31. Belfiore R, Rodin A, Ferreira E, Velazquez R, Branca C, Caccamo A, Oddo S (2018) Temporal and regional progression of Alzheimer's disease-like pathology in 3xTg-AD mice. Aging Cell:e12873
32. Braak HBraak E (1995) Staging of Alzheimer's disease-related neurofibrillary changes. Neurobiol Aging 16(3):271–278 discussion 278-284
33. Mirra SS, Heyman A, McKeel D, Sumi SM, Crain BJ, Brownlee LM, Vogel FS, Hughes JP et al (1991) The consortium to establish a registry for Alzheimer's disease (CERAD). Part II. Standardization of the neuropathologic assessment of Alzheimer's disease. Neurology 41(4):479–486
34. Tucker KL, Meyer M, Barde YA (2001) Neurotrophins are required for nerve growth during development. Nat Neurosci 4(1):29–37
35. Blanchard J, Wanka L, Tung YC, Cardenas-Aguayo Mdel C, LaFerla FM, Iqbal K, Grundke-Iqbal I (2010) Pharmacologic reversal of neurogenic and neuroplastic abnormalities and cognitive impairments without affecting Abeta and tau pathologies in 3xTg-AD mice. Acta Neuropathol 120(5):605–621
36. Carroll JC, Rosario ER, Kreimer S, Villamagna A, Gentzschein E, Stanczyk FZ, Pike CJ (2010) Sex differences in beta-amyloid accumulation in 3xTg-AD mice: role of neonatal sex steroid hormone exposure. Brain Res 1366:233–245
37. Clinton LK, Billings LM, Green KN, Caccamo A, Ngo J, Oddo S, McGaugh JL, LaFerla FM (2007) Age-dependent sexual dimorphism in cognition and stress response in the 3xTg-AD mice. Neurobiol Dis 28(1):76–82
38. Hirata-Fukae C, Li HF, Hoe HS, Gray AJ, Minami SS, Hamada K, Niikura T, Hua F et al (2008) Females exhibit more extensive amyloid, but not tau, pathology in an Alzheimer transgenic model. Brain Res 1216:92–103
39. Alonso AD, Grundke-Iqbal I, Iqbal K (1995) Bovine and human tau, highly homologous but less crossreactive: implications for Alzheimer disease. Brain Res Mol Brain Res 31(1–2):194–200
40. Tatebayashi Y, Iqbal K, Grundke-Iqbal I (1999) Dynamic regulation of expression and phosphorylation of tau by fibroblast growth factor-2 in neural progenitor cells from adult rat hippocampus. J Neurosci 19(13):5245–5254
41. Liu F, Iqbal K, Grundke-Iqbal I, Hart GW, Gong CX (2004) O-GlcNAcylation regulates phosphorylation of tau: a mechanism involved in Alzheimer's disease. Proc Natl Acad Sci U S A 101(29): 10804–10809
42. Pei JJ, Braak E, Braak H, Grundke-Iqbal I, Iqbal K, Winblad B, Cowburn RF (1999) Distribution of active glycogen synthase kinase 3beta (GSK-3beta) in brains staged for Alzheimer disease neurofibrillary changes. J Neuropathol Exp Neurol 58(9):1010–1019
43. Liu F, Zaidi T, Iqbal K, Grundke-Iqbal I, Merkle RK, Gong CX (2002) Role of glycosylation in hyperphosphorylation of tau in Alzheimer's disease. FEBS Lett 512(1–3):101–106
44. Goedert M, Spillantini MG, Crowther RA (1992) Cloning of a big tau microtubule-associated protein characteristic of the peripheral nervous system. Proc Natl Acad Sci U S A 89(5):1983–1987
45. Buee L, Bussiere T, Buee-Scherrer V, Delacourte A, Hof PR (2000) Tau protein isoforms, phosphorylation and role in neurodegenerative disorders. Brain Res Brain Res Rev 33(1):95–130
46. Lee VM, Balin BJ, Otvos L Jr, Trojanowski JQ (1991) A68: a major subunit of paired helical filaments and derivatized forms of normal Tau. Science 251(4994):675–678
47. Zhou Y, Shi J, Chu D, Hu W, Guan Z, Gong CX, Iqbal K, Liu F (2018) Relevance of phosphorylation and truncation of tau to the etiopathogenesis of Alzheimer's disease. Front Aging Neurosci 10: 27
48. Sjogren M, Davidsson P, Tullberg M, Minthon L, Wallin A, Wikkelso C, Granerus AK, Vanderstichele H et al (2001) Both total and phosphorylated tau are increased in Alzheimer's disease. J Neurol Neurosurg Psychiatry 70(5):624–630
49. Yin Y, Gao D, Wang Y, Wang ZH, Wang X, Ye J, Wu D, Fang L et al (2016) Tau accumulation induces synaptic impairment and memory deficit by calcineurin-mediated inactivation of nuclear

CaMKIV/CREB signaling. Proc Natl Acad Sci U S A 113(26): E3773–E3781

50. Wischik CM, Novak M, Edwards PC, Klug A, Tichelaar W, Crowther RA (1988) Structural characterization of the core of the paired helical filament of Alzheimer disease. Proc Natl Acad Sci U S A 85(13):4884–4888
51. Wischik CM, Novak M, Thogersen HC, Edwards PC, Runswick MJ, Jakes R, Walker JE, Milstein C et al (1988) Isolation of a fragment of tau derived from the core of the paired helical filament of Alzheimer disease. Proc Natl Acad Sci U S A 85(12):4506–4510
52. Guillozet-Bongaarts AL, Garcia-Sierra F, Reynolds MR, Horowitz PM, Fu Y, Wang T, Cahill ME, Bigio EH et al (2005) Tau truncation during neurofibrillary tangle evolution in Alzheimer's disease. Neurobiol Aging 26(7):1015–1022
53. Horowitz PM, Patterson KR, Guillozet-Bongaarts AL, Reynolds MR, Carroll CA, Weintraub ST, Bennett DA, Cryns VL et al (2004) Early N-terminal changes and caspase-6 cleavage of tau in Alzheimer's disease. J Neurosci 24(36):7895–7902
54. Zilka N, Filipcik P, Koson P, Fialova L, Skrabana R, Zilkova M, Rolkova G, Kontsekova E et al (2006) Truncated tau from sporadic Alzheimer's disease suffices to drive neurofibrillary degeneration in vivo. FEBS Lett 580(15):3582–3588